Temporally Resolved Measurement of Electron Densities ($>10^{23}$ cm^{-3}) with High Harmonics

W. Theobald, R. Häßner, C. Wülker,* and R. Sauerbrey

Institut für Optik and Quantenelektronik, Friedrich-Schiller-Universität Jena, Max-Wien-Platz 1, D-07743 Jena, Germany

(Received 22 February 1996)

It is shown experimentally that a high intensity subpicosecond laser impinging on a solid target generates a plasma with an electron density exceeding 10^{23} cm^{-3}. Depending on the electron density, femtosecond high-order harmonics from a gas jet are transmitted through a subpicosecond laser-produced plasma while lower order harmonics are absorbed or reflected. In the present experiment, electron densities up to 4.3×10^{23} cm^{-3} at mean electron energies of 50 to 150 eV are measured and the plasma expansion is mapped out in time with subpicosecond resolution. [S0031-9007(96)00538-8]

PACS numbers: 52.70.Kz, 42.65.Ky, 52.40.Nk, 52.50.Jm

With high intensity subpicosecond laser sources it has become possible to heat solids to mean electron energies of several 100 eV at almost constant ion density. Rapid ionization increases the density of free electrons and a dense plasma with an electron density exceeding solid density is generated. Much attention has focused on this new, unusual state of matter, and a number of experiments investigating the dynamics [1,2], laser coupling [3,4], x-ray emission [5,6], and nonlinear optics [7,8] of such dense plasmas generated by ultrashort laser pulses have been performed. In the interpretation of most of these experiments it was assumed that a solid density plasma was generated by the laser pulse. Plasma spectroscopy is to our knowledge the only method that can provide information about these dense plasmas [9]. Time averaged electron densities of up to 6×10^{23} cm^{-3} produced by subpicosecond laser pulse at an intensity of 10^{19} W/cm^2 were recently inferred from line profile measurements of Li-like Cl spectra [10]. By combining an x-ray spectrograph with an x-ray streak camera additional temporal resolution can be obtained. Densities of up to 8×10^{24} cm^{-3} and 60 ps time resolution are reported in [11] using this method. Electron densities up to 3.2×10^{21} cm^{-3} were measured with a technique based on Moiré interferometry using soft x-ray laser radiation [12].

In this paper we demonstrate a new experimental method that uses high harmonics generated by a subpicosecond laser pulse in a gas jet [13] as a probe for a solid density plasma generated in a thin foil by a second temporally correlated laser pulse. With this experiment it is shown directly that subpicosecond lasers produce solid density plasmas by measuring simultaneously both the electron density as well as the mean electron energy as a function of time with subpicosecond temporal resolution. The idea presented here is to measure the transmittance of a plasma at two or more different frequencies in such a way that some frequencies are below the plasma frequency while others are above. Light can propagate in a plasma with electron density $n_e < n_c$ where n_c is the critical density given by $n_c = 4\pi^2\varepsilon_0 m_e c^2/e^2\lambda^2 \approx 1.11 \times 10^{21}/(\lambda/\mu\text{m})^2$ cm^{-3}. From the ratio of the transmitted signal at the different frequencies one can obtain the electron density. The wavelength of the probe radiation for solid density plasmas has to be in the extreme ultraviolet (XUV) region. A convenient way to generate ultrashort pulse, high brightness XUV radiation is high-order harmonic generation in gases using ultrashort laser pulses. This method provides coherent light pulses down to a wavelength below 10 nm [14,15] corresponding to critical plasma densities of 10^{25} cm^{-3}, or about 1000 times solid density for a hydrogen plasma. The applications of such ultrashort XUV pulses are only just beginning [16] and offer unique possibilities to study the dynamics of extremely dense laser-produced plasmas. We have used high-order harmonics, in particular, the 5th (50 nm) and 7th (35 nm) harmonics, produced by subpicosecond KrF laser radiation [17] for direct and time-resolved measurement of electron density in a laser-produced plasma. A time-resolved measurement of the transmitted signals allows us to determine both the electron density with a precision of about 10%, and independently the mean electron energy with a somewhat lower precision.

The short-pulse laser consists for a hybrid dye–KrF excimer oscillator [18] and a KrF power amplifier. It operates with 1 Hz repetition rate and delivers pulses at a wavelength of 248.5 nm with a pulse duration of 0.7 ps. Figure 1 shows the setup of the experiment. Two temporally correlated pulses of 10 and 30 mJ energy, respectively, are generated. The 10 mJ pulse is used for the generation of a plasma while the 30 mJ pulse produces high-order harmonics acting as a probe beam. The experiment takes place in a large vacuum chamber of 1 m diameter evacuated to a pressure of $\sim 10^{-5}$ mbar. The pulse which produces the harmonics is focused by a $f/21$ plano convex CaF_2 lens with a focal length of $f = 120$ cm into a neon or helium gas jet of density 3×10^{17} cm^{-3} released by a piezoelectric drive pulsed valve. At an intensity of $3^{+2}_{-1} \times 10^{15}$ W/cm^2 harmonics up to the 13th order are detected in a single shot [17]. Their temporal duration is estimated to be less than 300 fs based on blueshift measurements of the third harmonic of KrF-laser radiation [19]. The second pulse is focused

 0031-9007/96/77(2)/298(4)$10.00

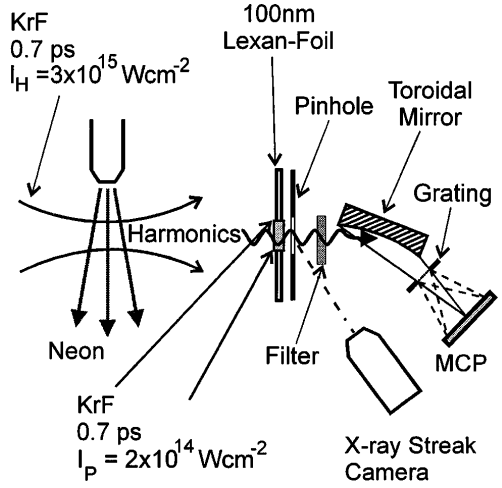

FIG. 1. Schematic of the experimental setup. From the left-hand side high-order harmonics created in a neon gas jet transmit a plasma generated by a correlated subpicosecond laser pulse in a 70–100 nm Lexan foil. A pinhole restricts the transmitted radiation subsequently detected by an soft x-ray spectrograph. An x-ray streak camera is used to align the temporal overlap of the two laser pulse.

by a $f/10$ plano convex lens with a focal length of 25 cm to a spot size of 70 μm on the surface of a 70–100 nm thick polycarbonate resin foil (Lexan 101, GE Plastics). The *p*-polarized light pulses with an intensity of $2^{+2}_{-1} \times 10^{14}$ W/cm^2 strike the target foil under an angle of incidence of 45°. Preplasma formation is not expected because the contrast ratio in these experiments was better than 10^7. The target foil is located 8 mm behind the gas nozzle so that the laser beam which creates the high-order harmonics illuminates an area of 700 × 400 μm^2. This gives an intensity of $\sim 10^{13}$ W/cm^2 of the fundamental on the foil. The linear absorption coefficient of Lexan increases from 35 up to 65 μm^{-1} in the wavelength region between 35 and 50 nm [20]. Therefore the transmittance decreases from 3% to 0.2% in a 100 nm thick foil and the Lexan strongly attenuates the harmonics. Only after creation of a plasma are the harmonics transmitted. A pinhole with 200 μm diameter is located 300 μm behind the foil to restrict the area from which the transmitted radiation is detected. A delay line in one of the beam paths equipped with a micrometer screw allows one to change the timing between the two pulses with a precision of about 60 fs. The zero time delay coarse alignment is performed by an x-ray streak camera within ±2 ps. This is refined by the pump-probe measurements itself to a precision of about 0.5 ps that is on the order of the pulse duration. For the detection of the high-order harmonics a single shot soft x-ray spectrograph with a spectral range from 10 to 700 Å is used [21]. A toroidal mirror performs a 1:1 imaging of the source onto the detector which consists of a microchannel plate (MCP) and a photodiode array. A free standing gold transmission grating (1000 lines per mm) acts as a dispersive element, and a 1.0 μm thick aluminum foil in front of the spectrograph blocks the fundamental so that only the XUV radiation is detected.

Figure 2 shows single-shot spectra of the 5th (50 nm) and the 7th (35 nm) harmonics transmitted through the plasma created in 100 nm thick Lexan foil at different time delays indicated in the figures. Part of the harmonic spectrum without the foil target is displayed in Fig. 2(a). A pinhole of 50 μm diameter was placed at the target position to determine the signal ratio at zero electron density The 5th harmonic appears about 3 times more intense than the 7th harmonic. At negative time delays, i.e., the harmonic pulse comes before the plasma is created, only plasma radiation visible as a background at all delay times is observed. Starting at zero delay [Fig. 2(b)] the seventh harmonic appears stronger than the fifth contrary to the spectra without plasma. With increasing delay [Fig. 2(c)–2(e)] the intensity ratio between the 7th and the 5th decreases until at 12 ps delay [Fig. 2(f)] almost the ratio without plasma is reached. Qualitatively this series of spectra shows the expected behavior: In case of the dense plasma [Fig. 2(b)] the high frequency (7th harmonic) is much better transmitted by the plasma than the lower frequency (5th harmonic). This ratio gradually changes while the plasma is expanding freely and the density decreases. For long times between the plasma creation and the appearance of the probe radiation the original ratio is almost recovered since a sufficiently thin plasma transmits both harmonics equally.

The absorption in the plasma can in principle be due to bound-bound, bound-free, and free-free transitions. In particular, absorption in CIII caused by the $2p$-$3d$ transitions has to be considered for the fifth harmonic. An estimate of the absorption coefficient α times length l yields $\alpha l < 10^{-2}$ under the present conditions. The contribution of bound-free absorption is estimated to be about 10 times smaller than free-free absorption, i.e., $\alpha_{ff}/a_{bf} \geq$

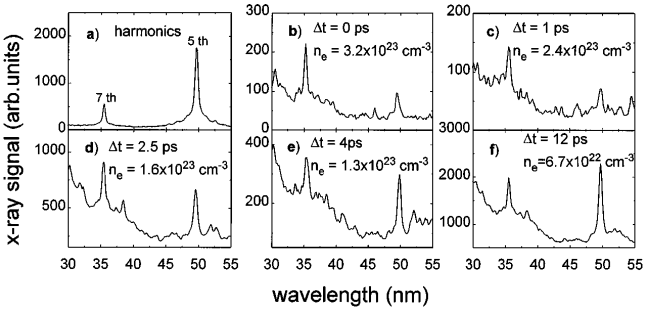

FIG. 2. Measured spectra of the 5th (50 nm) and the 7th (35 nm) harmonics transmitted at different time delays through a subpicosecond laser-produced plasma. (a) The harmonic spectrum without plasma. Starting from zero delay (b) the intensity ratio between the 7th and 5th decreases until almost the ratio without plasma is reached [2(c)–(f)]. The deduced electron densities are indicated in the figures (see text).

10. Only collisional heating is therefore further considered in the following analysis. The optical properties of the plasma may be described by the Drude model [22] leading to a complex dielectric constant $\varepsilon = n^2 = 1 - \omega_p^2/(\omega^2 + i\nu_c\omega)$, where n is the complex index of refraction, ω is the angular frequency of the electromagnetic radiation, and ν_c is the electron-ion collision frequency calculated for a Maxwellian velocity distribution in the free electron gas [22]. The probe radiation impinges perpendicular on the target surface and the Fresnel equations are used to calculate the transmitted part of the radiation passing through a strongly absorbing medium of thickness d with a spatially averaged electron density n_e. The complex index of refraction $n = n_{\text{real}} + in_{\text{imag}}$ is calculated, and afterwards the fraction of radiation reflected at the vacuum-plasma boundary is computed which can be written as $R = |(n - 1)/(n + 1)|^2$. The fraction absorbed in the plasma is given by $\exp(-\alpha d)$ with the linear absorption coefficient $\alpha = (4\pi/\lambda)n_{\text{imag}}$ where λ is the wavelength of the probe radiation. Considering that part of the radiation is backreflected at the rear density step the transmittance is then given by $(1 - R)^2 \exp(-\alpha d)$ neglecting multiple beam interference effects. It turns out that under the present conditions the transmitted probe radiation intensity is dominated by absorption. The reflected part does not exceed 20% for the 5th and 3% for the 7th harmonics. The assumption of a steep plasma gradient is therefore not critical for the quantitative results. Refraction of the harmonic radiation in the plasma due to a lateral density gradient has to be considered only for radial scale lengths shorter than 10 μm. The part of the radiation which is in this case refracted out of the acceptance angle of the spectrograph never exceeds 20% of the total transmitted radiation. This was taken into account in the uncertainty of the determined electron density.

It is now possible to calculate the transmitted signal of the 7th and 5th harmonics as a function of the electron density n_e. Figure 3(a) shows the ratio of the transmitted 7th to the transmitted 5th versus n_e for various mean electron energies indicated in the figure for an initial plasma thickness of 100 nm. For a time delay of -0.5 ps no harmonic contributions are detected, and therefore the plasma formation occurs between -0.5 and 0 ps. A ratio of 9.2 ± 3.3 for zero delay leads to an initial electron density between $n_{e0} = (3.2^{+0.2}_{-0.3}) \times 10^{23}$ to $(3.7^{+0.1}_{-0.2}) \times 10^{23}$ cm^{-3} depending only weakly on the mean electron energy. The determined density is about 20 times the critical density of KrF radiation.

When an intense ultrashort laser pulse strikes the target an overcritical plasma layer is formed at the foil surface and a supersonic electron thermal wave travels into the bulk material. A velocity of 1.8×10^7 cm/s is reported [23] for similar laser intensities and similar plasma conditions. Thus, the time for the ionization front to travel through the foil is about 0.5 ps which is shorter

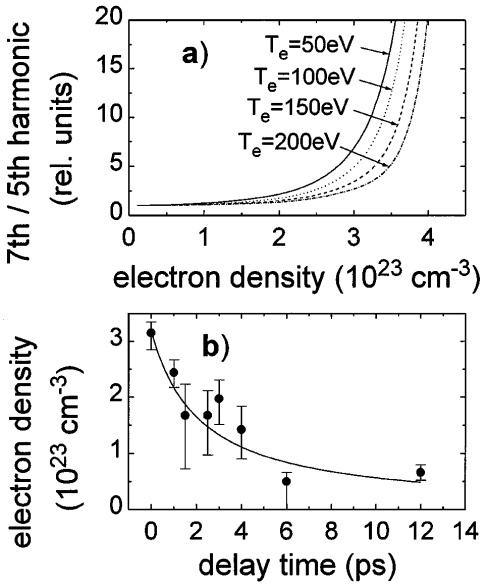

FIG. 3. (a) The calculated behavior of the transmitted harmonic signal ratio of the 7th to 5th versus electron density for zero time delay. The ambiguity of the determination of electron density and mean electron energy is removed by observing the time evolution of the electron density. (b) The measured decay of the electron density due to the expansion of the plasma and the calculation for an initial mean electron energy of 50 eV (solid line).

than the laser pulse duration (0.7 ps). After the laser pulse has ceased, the plasma undergoes an adiabatic expansion which, for the short delay times concerned here, we can assume to be a uniform planar expansion with constant velocity v of the two outer edges. The electron density is then given by $n_e = n_{e0}(d_0/d)$, where n_{e0} is the initial electron density, d_0 the initial thickness, and $d = d_0 + vt$ the thickness at later times. The mean electron energy develops in time according to $T = T_{e0}(d_0/d)^{\gamma-1}$, where T_{e0} is the initial mean electron energy and $\gamma = 5/3$ the adiabatic coefficient for a plasma. It is important to note that the time evolution of the ratio of the 7th to 5th harmonics is only a function of the initial electron density and the initial mean electron energy so that these two parameters are directly obtained from the measurement. The determination of the electron density in an expanding plasma is also affected by recombination. For delay times in excess of about 5 ps an additional decrease in electron density by at most a factor of 2 has been estimated assuming Saha equilibrium for the ionization.

The measured transmittance ratios versus time imply an initial mean electron energy of $T_{e0} \approx 50$ eV. We are now able to plot the electron density versus time as shown in Fig. 3(b). The initial plasma parameters ($\Delta t = 0$) are $n_{e0} = (3.2^{+0.2}_{-0.3}) \times 10^{23}$ cm^{-3}, $\langle Z \rangle = 3.8^{+0.2}_{-0.4}$, $T_{e0} \approx 50$ eV where $\langle Z \rangle$ is the average degree of ionization. The solid curve represents the calculated density decay. A charge state of $\langle Z \rangle = 3.4$ is expected from the Saha

equation at a temperature of 50 eV for a solid density carbon plasma. Lexan predominantly consists of carbon but has a somewhat lower solid state ion density of $8.5 \times 10^{22}\ \mathrm{cm}^{-3}$ compared to $1 \times 10^{23}\ \mathrm{cm}^{-3}$ for carbon yielding an estimated value of $\langle Z \rangle \approx 3$. A similar measurement with a foil of 70 nm thickness and laser intensity of about $5 \times 10^{14}\ \mathrm{W/cm}^2$ yielded a maximum electron density of $n_{e0} = (4.3^{+0.2}_{-0.3}) \times 10^{23}\ \mathrm{cm}^{-3}$ or $\langle Z \rangle = 5.1^{+0.2}_{-0.3}$. The measured density decay was faster than shown in Fig. 3(b) which implies a higher initial mean electron energy of $T_{e0} \approx 150$ eV consistent with the higher degree of ionization.

In summary, we have presented a simple method to measure both the evolution of the plasma free electron density above $10^{23}\ \mathrm{cm}^{-3}$ and the mean electron energy with subpicosecond time resolution capable of being extended to even higher densities.

Valuable discussions with Hans Griem are gratefully acknowledged. We also thank P. Mämpel for providing us with excellent foil targets.

*Present address: Laser Science Group, The Institute of Physical and Chemical Research (RIKEN), Hirosawa 2-1, Wako-shi, Saitama 351-01, Japan.

[1] H. M. Milchberg, R. R. Freeman, S. C. Davey, and R. M. Moore, Phys. Rev. Lett. **61**, 2364 (1988).

[2] J. Workman, A. Maksimchuk, X. Liu, U. Ellenberger, J. S. Coe, C. Y. Chien, and D. Umstader, Phys. Rev. Lett. **75**, 2324 (1995).

[3] U. Teubner, J. Bergmann, B. van Wonterghem, F. P. Schäfer, and R. Sauerbrey, Phys. Rev. Lett. **70**, 794 (1993).

[4] D. F. Price, R. M. More, R. S. Walling, G. Guethlein, R. L. Sheperd, R. E. Stewart, and W. E. White, Phys. Rev. Lett. **75**, 252 (1995).

[5] T. Ditmire, T. Donnelly, R. W. Falcone, and M. D. Perry, Phys. Rev. Lett. **75**, 3122 (1995).

[6] A. McPherson, B. D. Thompson, A. B. Borisov, K. Boyer, and C. K. Rhodes, Nature (London) **370**, 631 (1994).

[7] D. von der Linde, T. Engers, G. Jenke, P. Agostini, G. Grillon, E. Nibbering, A. Mysyrowicz, and A. Antonetti, Phys. Rev. A **52**, R25 (1995).

[8] S. Kohlweyer, G. D. Tsakiris, C.-G. Wahlström, C. Tillman, and I. Mercer, Opt. Commun. **117**, 431 (1995).

[9] Y. Leng, J. Goldhar, H. R. Griem, and R. W. Lee, Phys. Rev. E **52**, 4328 (1995).

[10] Z. Jiang, J. C. Kieffer, J. P. Matte, M. Chaker, O. Peyrusse, D. Gilles, G. Korn, A. Maksimchuk, S. Coe, and G. Mourou, Phys. Plasmas **2**, 1702 (1995).

[11] C. F. Hooper, Jr., D. P. Kilcrease, R. C. Mancini, L. A. Woltz, D. K. Bradley, P. A. Jaanimagi, and M. C. Richardson, Phys. Rev. Lett. **63**, 267 (1989).

[12] D. Ress, L. B. DaSilva, R. A. London, J. E. Trebes, S. Mrowka, R. J. Procassini, T. W. Barbee, Jr., and D. E. Lehr, Science **265**, 514 (1994).

[13] See, for example, A. L'Huillier, L.-A. Lompré, G. Mainfray, and C. Manus, in *Atoms in Intense Laser Fields*, edited by M. Gavrila (Academic Press, San Diego, 1992), p. 139.

[14] J. J. Macklin, J. D. Kmetec, and C. L. Gordon, III, Phys. Rev. Lett. **70**, 766 (1993).

[15] S. G. Preston, A. Sanpera, M. Zepf, W. J. Blyth, C. G. Smith, J. S. Wark, M. H. Key, K. Burnett, M. Nakai, D. Neely, and A. A. Offenberger, Phys. Rev. A **53**, R31 (1996).

[16] P. Balcou, P. Salières, K. S. Budil, T. Ditmire, M. Perry, and A. L. Huillier, Z. Phys. D **34**, 107 (1995).

[17] W. Theobald, C. Wülker, F. P. Schäfer, and B. N. Chichkov, Opt. Commun. **120**, 177 (1995).

[18] G. Almàsi, S. Szatmári, and P. Simon, Opt. Commun. **88**, 231 (1992).

[19] S. P. Le Blanc, Z. Qi, and R. Sauerbrey, Opt. Lett. **20**, 312 (1995).

[20] F. R. Powell, P. W. Vedder, J. F. Lindblom, and S. F. Powell, Opt. Eng. **29**, 614 (1990).

[21] J. Jasny, U. Teubner, W. Theobald, C. Wülker, J. Bergmann, and F. P. Schäfer, Rev. Sci. Instrum. **65**, 1631 (1994).

[22] W. L. Kruer, *The Physics of Laser Plasma Interactions* (Addison-Wesley, New York, 1988).

[23] B.-T. V. Vu, A. Szoke, and O. L. Landen, Phys. Rev. Lett. **72**, 3823 (1994).